Transactions, SMiRT-24
BEXCO, Busan, Korea - August 20-25, 2017
Division IX - Waste Management and Decommissioning

BACTERIAL EFFECTS ON MASS TRANSPORT IN POROUS MEDIA

Todor G. Baychev[1], Simon Gregory[2], Momtchil S. Tomov[3], Christopher Boothman[4], Andrey P. Jivkov[1] and Jonathan R. Lloyd[4]

[1] Modelling & Simulation Centre, School of Mechanical Aerospace & Civil Engineering, The University of Manchester, Oxford Road, Manchester M13 9PL, UK
[2] British Geological Survey, Keyworth, Nottingham NG12 5GG, UK
[3] Department of Neurobiology, Harvard Medical School, 220 Longwood Avenue, Goldenson Building, Boston, MA 02115, USA
[4] Williamson Research Centre for Molecular Environmental Science, School of Earth and Environmental Sciences, The University of Manchester, Oxford Road, Manchester M13 9PL, United Kingdom

ABSTRACT

Understanding and predicting fluid flow through porous media is of fundamental importance to the design and operation of a geological disposal facility. For example, bacterial colonisation in the vicinity of the facility could potentially introduce an additional barrier between the radioactive waste and biosphere, with reported cases of reduction of the hydraulic permeability of the media of up to 98% (Cunningham *et al.* 1991). In this work, we present results from a flow-through sandstone column experiment colonized by the bacterium *Pseudomonas aeruginosa* and discuss the effects on the permeability of the system. Results indicate that such systems are susceptible to perturbations and that it is possible to obtain fairly even biomass distribution throughout the core. The experiment duration was 2500 hours during which time the injection pressure increased nearly two orders of magnitude. In addition, we conducted two XCT scans of the Hollington sandstone at a range of resolutions and extracted the equivalent irregular pore network models. Based on these networks, we developed an approach for the identification of a small number of critical features, that if affected by bacterial colonisation, the permeability of the media could be affected dramatically. The modeling results show that if the size of the critical features is reduced to 25% of its original size, this could yield permeability reduction of up to 85%. The study demonstrates the key effect of the critical features to the hydraulic permeability and the potential for a small amount of biomass to influence mass transport in porous media significantly.

Keywords: Hollington sandstone, *Pseudomonas aeruginosa*, permeability, critical features, flow through column, biofilm, pore network modeling.

INTRODUCTION

Nuclear energy will continue to contribute to the global energy mix as energy demands increase with the world population. As any other industry it produces waste, however, in much smaller quantities than coal or gas. The internationally accepted route for disposal, including in the UK, of intermediate and highly radioactive waste is via a Geological Disposal Facility (GDF). The significance of bacterial communities in this scenario comes from the fact that they are potentially present or adjacent to virtually every engineered barrier in a GDF, as well as in the host geology. Their presence and effects on the system has not been studied in detail, and only recently they have been recognised as a potential fifth barrier (in addition to the immobilised waste form, the canister, the backfill material and the host rock) between the radioactive waste and the biosphere. Bacterial metabolic processes may lead to radionuclides

transport, retardation or immobilisation by pore space blockage and/or redox processes. This paper will focus on the mechanical aspects of blockage.

Modelling biofilm growth is one of the main tools used to improve the current understanding of the interactions between bacterial "biofilms" and the hydrodynamics of porous media. This approach can provide predictions that are difficult to observe experimentally over geological time scales. Biofilms are agglomerates of surface-associated cells enclosed in a matrix of extracellular polymeric substances (EPS). Numerous mathematical models have been developed in the past that attempt to describe biofilm development (Wanner and Gujer 1986, Tiwari and Bowers 2001, Wang and Zhang 2010, Rajabzadeh *et al.* 2015) but only some of them are directly applicable to porous media investigations due to associated computational costs. These models are usually based on the Monod equation (Wynn and Liehr 2001) which is a kinetic model of microbial growth. Often, these models describe biofilms as homogenous formations (i.e. treating the EPS, cells, entrapped particles, gas bubbles etc. as a whole), with uniform thickness which is not strictly the case (Stoodley *et al.* 1999). These models require the input of several parameters such as the maximum cellular growth rate, substrate diffusion coefficients, detachment rate etc. Some of these coefficients may be easier to quantify than others using experimental observations, however, calibrating these models for mixed microbial communities could be challenging. Single species biofilms are rarely observed in nature and multispecies biofilms behave differently to their single species counterpart. For example, James et al. (1995), reported that pure cultures of either *Klebsiella pneumoniae* or *P. aeruginosa* form biofilms of thickness 15 μm and 30 μm respectively, whereas biofilms containing both species are thicker (40μm). The mechanical properties of mixed community biofilms are also likely to be different and depend on other environmental factors such as the available nutrients, the system's hydrodynamics etc. (Zhao *et al.* 2013, Langer *et al.* 2014). Keeping in mind these limitations, mathematical models can be used to model biofilm growth, but this alone is not enough to predict interactions with the hydrodynamics in porous media.

Modelling hydrodynamic-biofilm interactions also requires a detailed description of the relevent porous media. Pore network modelling (PNM) is a pore space generalisation approach that can be used to represent the porosity of any porous medium (Xiong *et al.* 2016, Baychev *et al.* 2017a). It discretises the complex pore space into pores (usually represented with spheres) which are interconnected by throats of different sizes (depending on the application these can be cylinders, cuboids or prisms (Valvatne and Blunt 2004, de Jong 2006)). PNM has many advantages over the established direct approaches as it allows the evaluation of much larger volumes of material that would be computationally too expensive to attempt using traditional methods (Baychev *et al.* 2017b). Coupling PNM with a biofilm growth model could be used to study hydrodynamics-biofilm interactions in attempt to predict mass transport coefficients (Suchomel *et al.* 1998). One of the main assumptions involved in coupling the two processes is the criterion for cell attachment i.e. which pores/throats would host biofilm growth. Existing models assume either complete coverage of the whole PNM or a random distribution, the realism of which questionable. The general consensus on initial cell attachment is that the process tends to be entirely stochastic, however, if the local conditions are unfavourable the cells could quickly return back to the liquid or "planktonic" phase (Langer *et al.* 2014). Numerous studies have attempted to improve the current understanding of where biofilms develop and clog pores/throats, with theories suggesting preferential clogging of either small or large pore/throats (Torbati *et al.* 1986, Thullner *et al.* 2000) but the lack of in-situ observations of the process in real time has not allowed for any definitive conclusions. Once the biofilm establishes in a particular pore/throat its interactions with the flow are not static. As the biofilm of bacterial cells grows, it reduces the available pore space for the fluid to pass through and can ultimately lead to the dispersion of planktonic cells that could give rise to new colonies. Larger fragments from existing mature colonies might also detach (depending on the local environmental conditions) and cause blockages of smaller pore/throats downstream. All these phenomena need to be accounted for in order to realistically model biofilm growth in porous media.

The aim of this paper is to improve the current understanding of the interplay between bacteria and flow in porous media by presenting experimental data from a Hollington sandstone core colonised by *P. aeruginosa* and the resulting effects on permeability. In addition, we offer a methodology for the

identification of a small number of pore space features, called 'critical features', that if colonised or blocked by detached fragments of biofilm could cause substantial decreases in permeability. We discuss our experimental observations and link them to the concept of critical features.

METHODOLOGY

Microbiological Experiments

Flow Through Experiment

The flow experiment was set up using a core from the Hollington Sandstone Quarry (Sherwood Sandstone group) placed in a biological flow apparatus (BFA) as described in Wragg *et al.* (2013), except that the sandstone core was double autoclaved and a Rheodyne® 2-position 6-port Injector was fitted in-line between the inlet pressure transducer and the entry to the pressure vessel and sample, to allow the inoculation of the bacterial culture; see fig 1. The reservoir (injection pump) was filled with a sterile artificial groundwater solution containing 14.6g NaCl, 0.25g sodium acetate and 1 ml of trace element solution SL-10(Widdel *et al.* 1983) and made up to 1l with deionised water. The experiment was run at 20 ˚C, and the flow from the reservoir, via an injection pump, was set at 200 µl h^{-1}. The experiment was inoculated after 527h with a culture of *Pseudomonas aeruginosa* (grown overnight LB broth (37˚C) and washed twice in artificial groundwater). 1ml of culture containing 7 x10^7 cells ml^{-1} was inoculated via the Rheodyne injector.

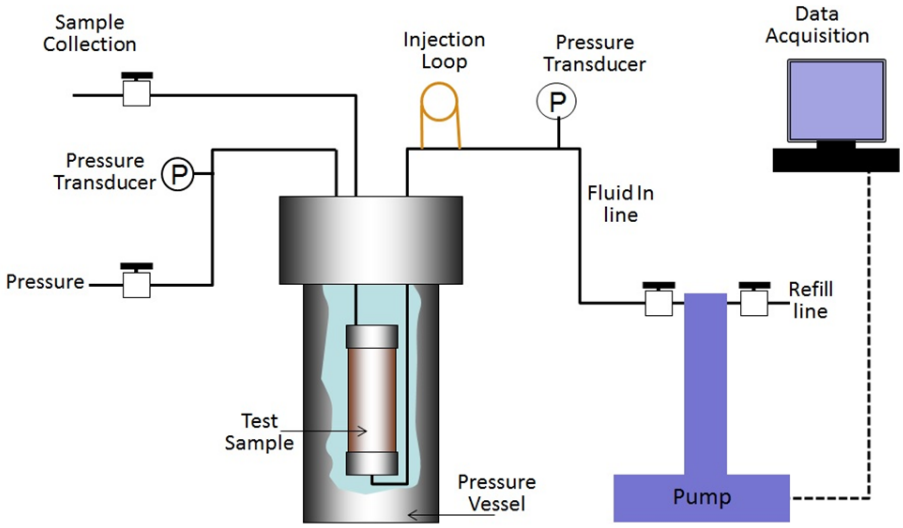

Figure 1.Experimental set-up.

Biomass Distribution: Standard Curve And Quantitative PCR Analysis

In order to extract bacterial DNA to allow the quantification of microbial colonisation, the sandstone core was removed from the biological flow apparatus and sliced transversely into 5 equally sized cylinders. Each sample was then crushed to facilitate the DNA extraction, which was performed from 0.25g of crushed sample using the Powerlyzer Powersoil Kit (Cambio, Cambridge, U.K.). To determine DNA abundance, QPCR was carried out using the Brilliant II SYBR Green QPCR reagents (Agilent Technologies). A serial dilution series of QPCR standards was prepared using a gBlock double stranded DNA gene fragment (Integrated DNA Technologies, Leuven, Belgium) covering nucleotide positions 1-570 of the 16S rRNA gene from species *Telluria mixta* DSM 4832. QPCR amplification was performed using a reaction mixture containing 12.5µl Brilliant II SYBR Green QPCR Master Mix, 2µl

DNA and 0.15µM of each primer in a 25µl final reaction volume. Amplification of the qPCR product was achieved using MX3000P QPCR system with a protocol including an initial step of 94ºC for 10 minutes followed by 30 cycles of 94ºC for 30 seconds, 50ºC for 30 seconds, 72ºC for 45 seconds. A dissociation curve was run between 94ºC and 50ºC to check the primer specificity, and the Ct value was determined automatically by the instrument. The standard curve for the qPCR reaction was created by plotting the cycle threshold (Ct) values of the dilution series against the log input of a DNA template. Concentrations ranging from 1.02ng μl^{-1} to 10.2fg μl^{-1} were used to generate the standard curve. All samples were analyzed in triplicate and the r^2 value for the QPCR run was 0.996.

The identities of the organisms comprising the microbial community within the sandstone core was determined by sequencing the PCR amplicons using an Illumina MiSeq platform (Illumina, San Diego, CA, USA) targeting the V4 hyper variable region of the 16S rRNA gene.

XCT Samples And Irregular Pore Network Extraction

The model porous medium used in this study is Hollington sandstone. The material has no particular relevance to the GDF but its high porosity (15-20%) makes it an attractive choice for conducting flow through experiments. Two XCT scans were conducted at a range of resolutions in order to quantify the pore space of the sandstone. The course resolution scan was performed on a sample (Sandstone L) of approximately 1 cm^3 using Nikon Custom Bay CT system. The voxel size obtained was 8.35 µm, which translates to a spatial resolution of around 25 microns. The fine resolution imaging was conducted on a sample (Sandstone H) of approximate dimensions of 1 x 2 mm, using a Zeiss Versa XRM-520 CT system. The voxel size obtained was 1.42 microns with a corresponding spatial resolution of around 4.3 microns. After reconstruction the data from both scans was loaded into Avizo standard 7.0 (Visualization Sciences Group, Bordeaux (VSG), France) for sub-volume extraction and segmentation. For Sandstone L the extracted subvolume is 400x400x400 voxels whereas for the Sandstone H is 350x350x350 voxels. Both sub volumes were extracted from the interior of the samples in order to minimise any effects on the microstructure from sample preparation. The extracted sub volumes underwent non-local means filtering, prior to segmentation. This was done manually by inspecting grey scale values along the transverse and longitudinal slices of the specimens. The resultant segmented samples contained only two phases: pore space and solid phase.

In order to convert the segmented samples into irregular pore network models (IPNM) we utilised the Watershed algorithm (Rabbani *et al.* 2014). The algorithm interprets the pores as spheres and the interconnecting throats as cylinders. As an output the algorithm provides pore coordinates and sizes as well as throat diameters and lengths and a list of interconnected pores. For more information about the scanning parameters, reconstruction and the method used for evaluating the pore network single-phase flow permeability refer to (Baychev *et al.* 2017a).

Critical Features Identification

We define a set of critical throats as any set of throats that has the following two properties:

1) clogging all throats in the set will render the PNM impermeable along a given axis, and
2) there is no smaller set of throats that has the above property. In that sense, a set of critical throats is minimal.

Intuitively, one can see why critical throats might be important (see fig 2). A large set of critical throats would imply that there are many non-overlapping paths that can sustain flow across the medium. Conversely, a small set of critical throats would suggest that there are bottlenecks in the media and that its permeability may be sensitive to their sizes. We can define a set of critical pores in a similar fashion.

Finding a set of critical throats is isomorphic to finding a minimum cut in a graph with vertices and edges corresponding to the PNM pores and throats, respectively. This is a standard problem in optimization theory and we solved it using the Edmonds-Karp algorithm (Cormen *et al.* 2009) and the max-flow min-cut theorem (Elias *et al.* 1956). Note that a PNM can have multiple sets of critical pores

and critical throats. While enumerating all such sets is computationally intractable, it is straightforward to find one set by performing breadth-first search on the residual flow network. Thus we found one set of critical pores and one set of critical throats for each IPNM that we used in all manipulations. For more details on the critical features refer to Baychev et al. (2017b).

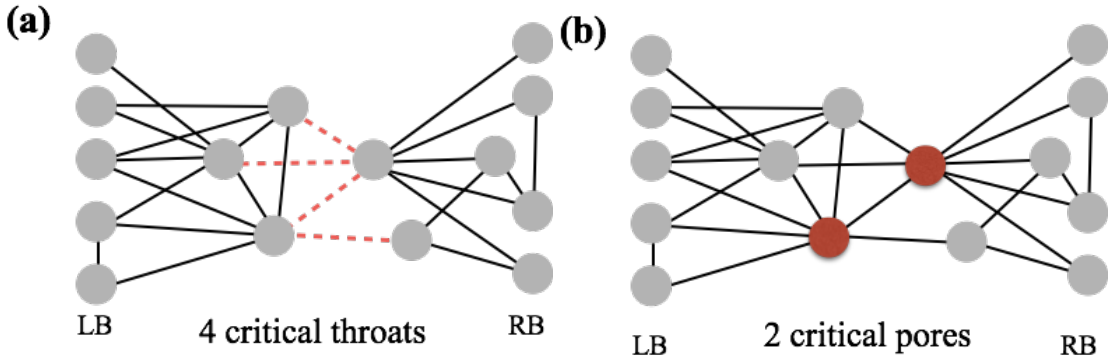

Figure 2. 2D representation of an IPNM. The flow is assumed to go from the left boundary (LB) and exiting the network from the right boundary (RB). Critical features are highlighted in red. **(a)** Example of a set of 4 critical throats **(b)** Example of a set of 2 critical pores

RESULTS

Pressure Variations

Since the flow through system was set to a constant flow rate and all other system parameters (viscosity and geometry) were relatively constant, any pressure fluctuations are directly indicative of the permeability of the rock core. From the start of the experiment until inoculation (~527h), no significant changes in permeability were observed, apart from a small pressure peak at around 280h, which is potentially the result of fine particles redistributing within the core. Almost immediately after inoculation, the injection pressure steadily increased for the following 53 h, reaching 111 kPa. During the period 581-800h, the injection pressure rapidly fluctuated between 29 kPa and 166 kPa, with an average of 117 kPa. This is potentially due to the planktonic bacteria travelling though the core and blocking critical pathways, followed by unblocking events due to increased local injection pressures. After 800h since the beginning of the experiment, the system stabilised for the next 720 h, after which the flow was stopped to refill the groundwater reservoir. The refill caused a sudden increase in the injection pressure to 260 kPa. On resuming the flow, the injection pressure did not restore to its previous levels, starting from 70 kPa and increasing to 244 kPa at 1910h. Following that, a failure in the microcontroller for nearly 24 h resulted in no records of the injection pressure. At 1938 h the pressure restored close to its previously recorded value (257 kPa). For the next 48 h the system had an electrical failure, which resulted in no flow passing through the core. The core inlet and outlet were sealed to prevent depressurising the system. Upon restoration of flow through the core, the injection pressure suddenly dropped to 150 kPa, which was then followed by steady increase to nearly 400 kPa before terminating the experiment, see fig 3. On decommissioning the experiment, no obvious signs of preferential flow between the Teflon sleeve and the core were observed, nor any visible signs of bacterial growth on the frits prior and after the core observed.

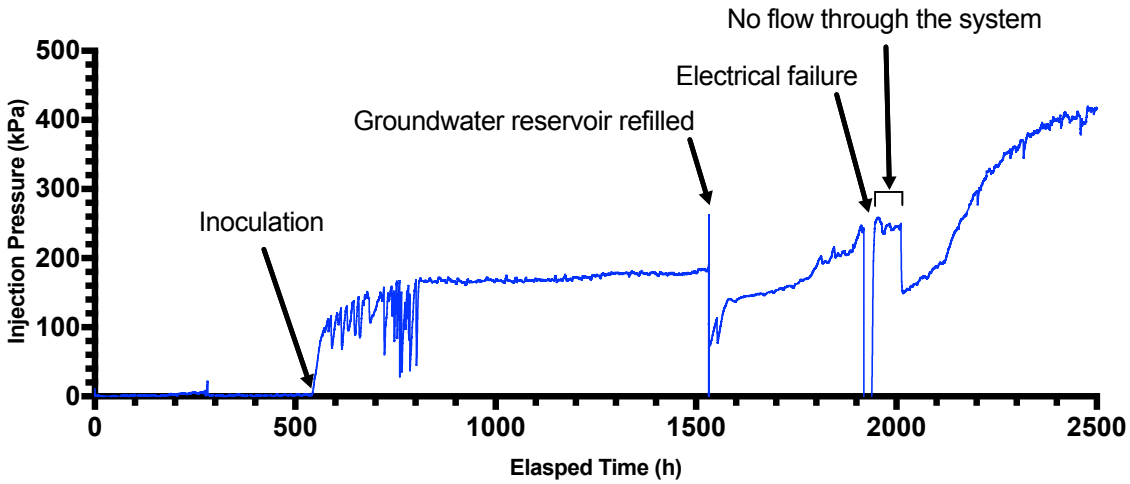

Figure 3. Injection pressure for the biotic column experiment.

Biomass Distribution

The DNA sequencing and qPCR analyses on the segmented core shows the key members of the bacterial community present and the relative abundance of DNA in each of the segments respectively, see fig 4. The biomass distribution shows no preferential colonisation of the inlet, with the biomass relatively evenly distributed throughout the length of the core. The results show that a number of other species besides the model bacteria are present, but it remains unclear whether the bacteria were viable at the end of the experiment, or whether DNA from dead cells was detected. It is plausible that the core was not completely sterile prior to inoculation, despite autoclaving, which allowed other organism to compete with *P. aeruginosa* near the outlet of the core. This could explain why the model bacteria are least abundant in sample 5.

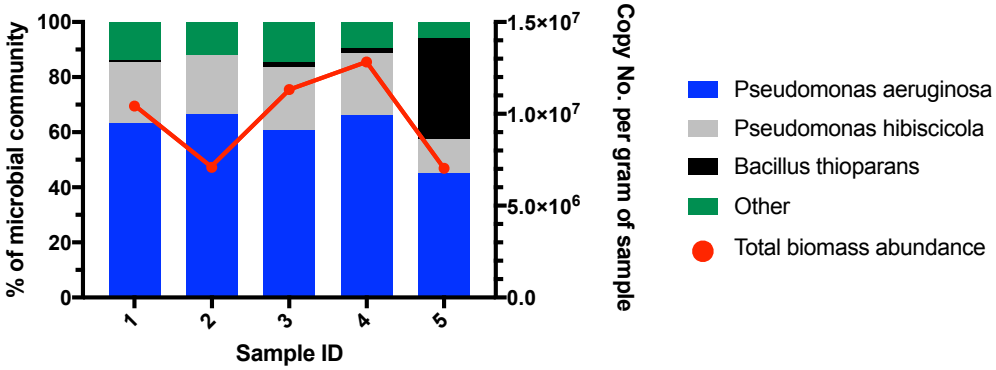

Figure 4. Biomass distribution in the core at ~2500h. Sample 1 is the inlet and sample 5 is the outlet of the core, relative to the flow direction.

Effect Of Critical Throats On IPNM Permeability

The radii of the critical throats along each principle direction were reduced by 50% and 75% of their original size, in order to assess the potential influence of biofilm developing in these throats. The rest of the pore space features are left unchanged. The effects on permeability are calculated based on steady state single-phase flow approach. The total number of throats present in Sandstone H and Sandstone L IPN models is 4723 and 7687 respectively. The maximum effect on permeability is observed with Sandstone H along the Y principle direction (58% reduction) when the size of 25 critical throats is

reduced by 75% of their original radii, see fig 5. Note that sample Sandstone L is not permeable in the X principle direction. The observed reductions in permeability are not monotonic due to the fact that various throats may have different lengths. No apparent link is observed between the number of critical throats and the induced permeability reduction.

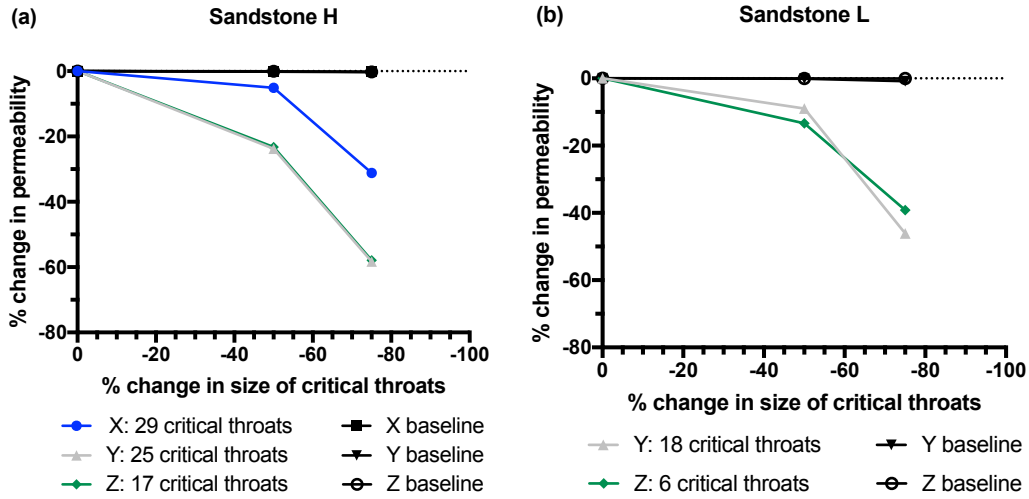

Figure 5. Effects of reducing the size of the critical throats on IPNMs permeability. Baseline results show the induced permeability change due to varying the sizes of the same number but randomly selected throats. **(a)** Sandstone H **(b)** Sandstone L. Note that the sample is not permeable in the X direction.

Effect Of Critical Pores On IPNM Permeability

Similar to the critical throats, the radii of the critical pores along each principle direction were reduced by 50% and 75% of their original size in order to assess the potential influence of biofilm developing in these pores. The IPNMs of Sandstone H and Sandstone L contain 2307 and 8406 pores respectively. The largest decrease in permeability (85%) is observed with Sandstone H along the Z principle direction, see fig 6. Note that the potential effects on permeability due to critical pores colonisation are likely to be more significant than the effect of the critical throats. A single pore could interconnect hundreds of throats and a potential blockage would affect them as well. The permeability along the principle directions with the least number of critical pores tend to be affected most by the size reductions, however, these results are not statistically representative due to the small number of analysed samples.

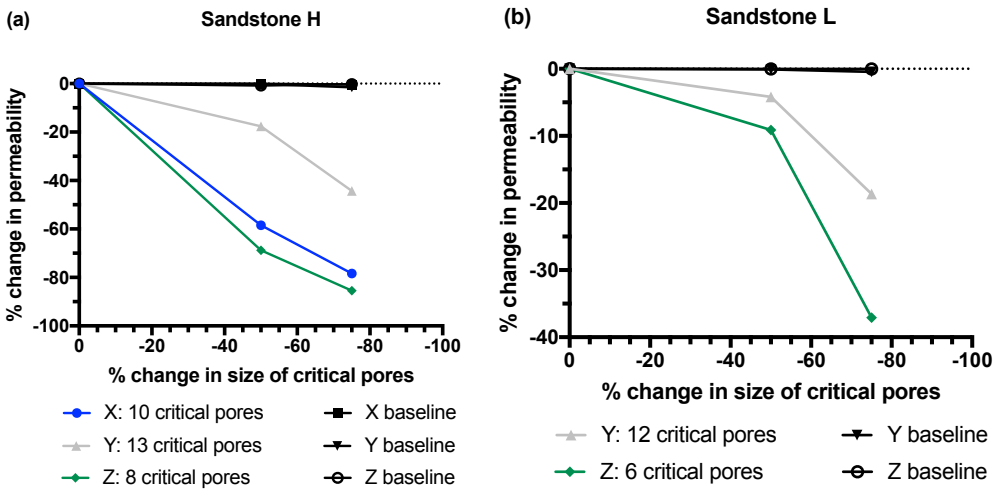

Figure 6. Effects of reducing the size of the critical pores on IPNMs permeability. Baseline results show the induced permeability change due to varying the sizes of the same number but randomly selected pores. **(a)** Sandstone H **(b)** Sandstone L. Note that the sample is not permeable in the X direction.

DISCUSSION

The flow-through column experiment demonstrated the complexity of the interactions between hydrodynamics in porous media and biofilm colonisation. The injection pressure showed four characteristic profiles: 'saw-tooth' like sudden oscillations, long periods of constant pressure, sudden drops and gradual increases. In order to model this behaviour we need an understanding of the mechanisms that lead to these pressure profiles. However, the inability to directly observe the processes at an appropriate spatial resolution makes it difficult to draw any definitive conclusions. The saw-tooth pressure changes, observed after inoculation, have been reported previously by Wragg et al. (2012) using a similar experimental set-up, however, they observed this phenomenon throughout the duration of the experiment (~6 months). A key difference between the two experiments is the fact that in the previous study the groundwater reservoir was inoculated, whereas in this study we injected the bacterial culture at a single time point directly prior to the core. The bacterial transfer time through the core is between 1-2 weeks, which coincides with the onset of the steady state pressure readings. Colloidal blocking and unblocking events of the critical features could explain this pressure profile, as simulations demonstrated that a small amount of biomass could induce rapid changes in permeability. Wragg et al. potentially observed the saw-tooth pressure fluctuations for extended periods of time because their system was constantly inoculated with the microbes growing in the groundwater reservoir. The equilibrium in injection pressure observed for over 4 weeks is interesting as it has not been observed before (to the best of our knowledge) and implies that any growth in the core was compensated by the detachment rate of bacteria. Furthermore, the detached fragments were not sufficiently large or as numerous to cause any simultaneous blockages of the critical features. Moreover, our experimental data demonstrated that the system is susceptible to perturbations, which in our case may have facilitated the colonisation of the core and decreased the permeability of the system. Refilling the ground water tank seems to have increased injection pressure, which could have sheared off some of the existing biofilm formations and accounted for the subsequent pressure drop. A study conducted with a biofilm of *P. fluorescens* growing in a pipe suggested that the shear strength of a biofilm is dependent on the initial flow conditions the colony developed in (Chen *et al.* 1998). Additionally, the lack of flow in the core for nearly 48 h may have led to starvation of some of the existing colonies and allowed for enhanced upstream chemotaxis to take place. The injection pressure dropped by 94 kPa upon flow restoration. Such a sharp and instantaneous pressure drop could be explained by starvation of colonies occupying a set of critical features. Such colonies

would have been previously exposed to a high flux of nutrients and upon flow termination were unable to sustain their population. Starvation in *P. aeruginosa* biofilms has been shown to increase alginate lyase expression which decreases the alginate and increases detachment (Boyd and Chakrabarty 1994). Following these events, the pressure increased steadily until the end of the experiment, reaching nearly two orders of magnitude increase in the injection pressure prior to inoculation.

The qPCR analysis on the segmented core indicates fairly even distribution of the biomass with a number of species present. The majority of previous experiments reported preferential clogging near the inlet of the columns. The perturbations and long time period over which the experiment took place may have facilitated the colonization of the system. Detached fragments of existing biofilm could shift the biomass distribution further downstream and the lack of flow for 2 days would potentially allows for bacteria to proliferate upstream as well as downstream due to nutrient gradients.

This experimental study has outlined some of the plausible explanations for the observed pressure readings, while the steady state simulations have highlighted the possible reductions in permeability if a set of critical features is to be blocked or colonised by biofilm. Whether the critical features are indeed favorable locations for bacterial colonies to establish requires further investigations. However, following the definition of critical features, all flow that passes though the sample is bound to pass though them, exposing them to the planktonic cells and all the nutrients that have not been consumed upstream. They may prove to be particularly favorable locations in nutrient poor environments as they are characteristic of high nutrient flux compared to any other non-critical pore or throat in the system, provided that the flow shear stress allows for cell attachment and colony development. In order to improve the current modeling approaches, a better understanding of where bacteria establish in porous media is needed, as well as how different environmental factors and community composition affect the shear strength of biofilm.

CONCLUSIONS

A flow-trough sandstone column experiment showed that *P. aeruginosa* can survive and develop in a saline environment. Over the course of the experiment, the injection pressure showed four different characteristic pressure profiles, including an equilibrium state, which was observed for over 4 weeks. The results indicate that the system is susceptible to perturbations and that it is possible to achieve an even biomass distribution throughout the porous media. The injection pressure increased by two orders of magnitude for the duration of the experiment (~2500h), showing that biofilm formation can significantly reduce the permeability of porous media. Numerical analysis on XCT scans of Hollington sandstone show the presence of small number of pore-space features, that we call ‘critical features’ that upon colonisation or blockage can significantly influence the permeability of the porous media. In order to improve the current modelling of biofilm induced clogging, we need a better understanding of the interplay between the bacteria and the critical features, as well as to what factors affect the shear strength of biofilms as this predetermines the dynamics of the system.

REFERENCES

Baychev, T. G., Jivkov, A. P., Rabani, A., Raeini, A. Q., Xiong, Q., Lowe, T. and Withers, P. J. (2017a) "Topological and Geometric Characterisation of Porous Media Part I: Experimental characterisation and irregular pore network modelling" - under review.

Baychev, T. G., Tomov, M. S., Jivkov, A. P. and Withers, P. J. (2017b) "Topological and Geometric Characterisation of Porous Media Part II: Homogenisation via regular pore network modelling" - under review.

Boyd, A. and Chakrabarty, A. M. (1994) "Role Of Alginate Lyase In Cell Detachment Of Pseudomonas Aeruginosa", *Applied and Environmental Microbiology*, 60(7), 2355-2359.

Chen, M. J., Zhang, Z. and Bott, T. R. (1998) "Direct measurement of the adhesive strength of biofilms in pipes by micromanipulation", *Biotechnology Techniques*, 12(12), 875-880.

Cormen, T. H., Leiserson, C. E., Rivest, R. L. and Stein, C. (2009) *Introduction to Algorithms*, The MIT Press; 3rd edition (July 31, 2009).

Cunningham, A. B., Characklis, W. G., Abedeen, F. and Crawford, D. (1991) "Influence Of Biofilm Accumulation On Porous-Media Hydrodynamics", *Environmental Science & Technology*, 25(7), 1305-1311.

de Jong, G. D. (2006) "Longitudinal and Transverse Diffusion in Granular Deposits", *Soil Mechanics and Transport in Porous Media: Selected Works of G. De Josselin De Jong*, 19, 260-267.

Elias, P., Feinstein, A. and Shannon, C. E. (1956) "A Note On The Maximum Flow Through A Network', *Ire Transactions on Information Theory*, 2(4), 117-119.

James, G. A., Beaudette, L. and Costerton, J. W. (1995) "Interspecies Bacterial Interactions In Biofilms", *Journal of Industrial Microbiology*, 15(4), 257-262.

Langer, S., Schropp, D., Bengelsdorf, F. R., Othman, M. and Kazda, M. (2014) "Dynamics of biofilm formation during anaerobic digestion of organic waste", *Anaerobe*, 29, 44-51.

Rabbani, A., Jamshidi, S. and Salehi, S. (2014) "An automated simple algorithm for realistic pore network extraction from micro-tomography images", *Journal of Petroleum Science and Engineering*, 123, 164-171.

Rajabzadeh, A. R., Legge, R. L. and Weber, K. P. (2015) "Multiphysics modelling of flow dynamics, biofilm development and wastewater treatment in a subsurface vertical flow constructed wetland mesocosm", *Ecological Engineering*, 74, 107-116.

Stoodley, P., Boyle, J. D., DeBeer, D. and Lappin-Scott, H. M. (1999) "Evolving perspectives of biofilm structure", *Biofouling*, 14(1), 75-+.

Suchomel, B. J., Chen, B. M. and Allen, M. B. (1998) "Macroscale properties of porous media from a network model of biofilm processes", *Transport in Porous Media*, 31(1), 39-66.

Thullner, M., Zeyer, J. and Kinzelbach, W. (2000) "Influence of microbial growth on hydraulic properties of pore networks", *Groundwater 2000*, 45-46.

Tiwari, S. K. and Bowers, K. L. (2001) "Modeling biofilm growth for porous media applications", *Mathematical and Computer Modelling*, 33(1-3), 299-319.

Torbati, H. M., Raiders, R. A., Donaldson, E. C., McInerney, M. J., Jenneman, G. E. and Knapp, R. M. (1986) "Effect Of Microbial Growth On Pore Entrance Size Distribution In Sandstone Cores", *Journal of Industrial Microbiology*, 1(4), 227-234.

Valvatne, P. H. and Blunt, M. J. (2004) "Predictive pore-scale modeling of two-phase flow in mixed wet media", *Water Resources Research*, 40(7).

Wang, Q. and Zhang, T. Y. (2010) "Review of mathematical models for biofilms", *Solid State Communications*, 150(21-22), 1009-1022.

Wanner, O. and Gujer, W. (1986) "A Multispecies Biofilm Model", *Biotechnology and Bioengineering*, 28(3), 314-328.

Widdel, F., Kohring, G. W. and Mayer, F. (1983) "Studies On Dissimilatory Sulfate-Reducing Bacteria That Decompose Fatty-Acids .3. Characterization Of The Filamentous Gliding Desulfonema-Limicola Gen-Nov Sp-Nov, And Desulfonema-Magnum Sp-Nov", *Archives of Microbiology*, 134(4), 286-294.

Wragg, J., Harrison, H., West, J. M. and Yoshikawa, H. (2012) "Comparison of microbiological influences on the transport properties of intact mudstone and sandstone and its relevance to the geological disposal of radioactive waste", *Mineralogical Magazine*, 76(8), 3251-3259.

Wynn, T. M. and Liehr, S. K. (2001) "Development of a constructed subsurface-flow wetland simulation model", *Ecological Engineering*, 16(4), 519-536.

Xiong, Q. R., Baychev, T. G. and Jivkov, A. P. (2016) "Review of pore network modelling of porous media: Experimental characterisations, network constructions and applications to reactive transport", *Journal of Contaminant Hydrology*, 192, 101-117.

Zhao, K., Tseng, B. S., Beckerman, B., Jin, F., Gibiansky, M. L., Harrison, J. J., Luijten, E., Parsek, M. R. and Wong, G. C. L. (2013) "Psl trails guide exploration and microcolony formation in Pseudomonas aeruginosa biofilms", *Nature*, 497(7449), 388-+.